Optimal Infrastructure Planning for EVs Fast Charging Stations based on Prediction of User Behavior

Gjelaj, Marjan; Toghroljerdi, Seyedmostafa Hashemi; Andersen, Peter Bach; Træholt, Chresten

Published in:
I E T Electrical Systems in Transportation

Link to article, DOI:
10.1049/iet-est.2018.5080

Publication date:
2019

Document Version
Peer reviewed version

Optimal Infrastructure Planning for EV Fast-Charging Stations Based on Prediction of User Behaviour

Marjan Gjelaj, Seyedmostafa Hashemi, Peter Bach Andersen, Chresten Træholt
Department of Electrical Engineering, Technical University of Denmark, 2800 Kgs. Lyngby, Denmark
margje@elektro.dtu.dk

Abstract: Electric vehicles (EVs) appear to offer a promising solution to support sustainable transportation and the reduction of CO_2 emissions in the metropolitan areas. To satisfy the EV load demand of the new EV models with larger battery capacities, public direct-current fast-charging stations (DCFCSs) are essential to recharge EVs rapidly. A stochastic planning method of the DCFCSs is presented considering user behaviour and the probabilistic driving patterns in order to predict EVs charging demand. According to the stochastic method, a coordinated charging demand and storage charging demand are proposed with the objective of minimising peak load from EVs and charging-infrastructure costs. The proposed planning method can prevent additional grid reinforcement costs due to EV demand during the peak hours. In the coordinated charging demand, the peak load from EVs is managed by controlling the DCFCSs. Instead, in the battery energy storage (BES) charging demand, an optimal BES is proposed as an alternative solution to reduce the peak demand of EVs as well as DCFCSs operational costs. Finally, an economic analysis is carried out to evaluate the technical and economic aspects related to DCFCSs, the BES life-cycle costs as well as the financial performance of BES costs versus grid reinforcement costs.

Nomenclature

Abbreviations

AC	Alternating Current
BES	Battery Energy Storage
B/C	Benefit-Cost ratio
BMS	Battery Management System
CBA	Cost-Benefit Analysis
CCS	Combined Charging System
DC	Direct Current
DSO	Distribution System Operator
DCFCS	DC Fast-Charging Station
DNTS	Danish National Transport Survey
EV	Electric Vehicle
IEC	International Electrotechnical Commission
ICE	Internal Combustion Engine
LV	Low Voltage
LTO	Lithium Titanate Oxide battery
MV	Medium Voltage
NPV	Net Present Value
NMC	Nickel Manganese Cobalt battery
PDF	Probability Density Function
PS	Peak Shaving
PBP	Payback Period
SoC	State of Charge
SD	Standard Deviation
V2G	Vehicle to Grid

Parameters

B	Benefit [€]
C	Costs [€]
E	Energy [kWh]
EV_D	EV demand [kWh]
EV_r	Electric Vehicle range [km]
EV_{mp}	EV maket penetration [%]
ICE_r	ICE vehicle range [km]
K	BES cycles
P	Power [kW]
T	Investment life
V_{ec}	EV consumption [kWh/km]
d	Driving distance [km]
t	time
l_n	PFD logarithmic distribution
η	Efficiency
μ	Mean
σ	Standard deviation
τ	EV charging time
α	DCFCS charging power setting
β	DCFCS charging duration setting
γ	DCFCS power and charging duration setting

1. Introduction

MANY European cities consider introducing driving restriction for diesel vehicles in and around metropolitan areas [1]. Electric vehicles (EVs) are a smart alternative to replace traditional vehicles in order to support sustainable transportation. For this reason, the demand for EV charging is expected to increase rapidly and could lead to load congestion in power systems [2].

This increase in EVs' penetration is an essential aspect of the planning for EVs charging infrastructures, in particular on the use of direct-current fast-charging stations (DCFCSs). Several studies have been carried out to analyse the possible impact of EVs on power systems considering various planning methods. The authors of [3] proposed an optimal location of the charging stations by taking into account the power transmission grid. Alternatively, [4] recommended a prediction method based on the energy-equivalent model for both centralised and decentralised charging loads. In addition, the authors of [5] suggested a multi-objective collaborative planning strategy in order to minimise the annual cost of investments in EV charging systems. Likewise, [6] proposed an optimal approach for sizing and siting fast-charging stations in order to reduce the infrastructure costs. The

authors of [7] exanimated the EV charging demand using demand-response programs and uncertainty problems.

Differently, [8] considered travel distance using a probabilistic model of EV charging loads. Similary, [9] used statistical data to establish a multi-objective EV charging planning model, with the goal of maximising captured traffic flow.

Another popular method for generating the EV load profiles involves Monte Carlo' simulations. The authors of [10] proposed a stochastic method in which Monte Carlo' simulations are used to calculate the EVs' arrival times and state of charge (SoC). Monte Carlo simulations in combination with Markov modelling can be used to statistically examine EVs, regardless of whether they are moving or parked. The stochastic method replicates different observations such as time of day, day of week and the driving patterns. Using this probabilistic method, it is possible to estimate the expected EV load profile using stochastic individual driving behaviour as a time-dependent function of the number trips and the driving distance. Likewise, [11] proposed to use the Markov chain in order to calculate the EV charging times. The Monte Carlo samples of driving patterns use discrete-times and states according to Markov chains [12]. In this framework, several states are defined (e.g., parked in a residential area, parked in a commercial area or in transit) [13]. Consequently, it is essential to predict the DCFCSs load demand.

In addition, the DCFCSs add a high-power consumption load that the distribution system operators (DSOs) must consider [14]. The impact of the DCFCSs such as generation planning [15], distribution transformers under different penetration levels [2] the aggregated EV charging demand [16], distribution network losses [17] and voltage drops have been investigated and analysed [18]-[19].

EVs have a serious impact on the grid, including various aspects of power systems; for example distribution transformers can become overloaded during peak hours [20], causing violations in voltage constraints [21]-[22]. To resolve these issues, for instance, large-scale vehicle-to-grid (V2G) can provide energy storage as part of the power grid by offering spinning reserves and regulating frequency through aggregators [23]. Likewise, [24] suggested V2G for ancillary services in particular frequency regulation and peak shaving (PS) by using a large fleet of EVs. V2G has demonstrated the potential to mitigate the negative grid impact of EVs by controlling DCFCSs during the charging and discharging processes. Alternatively, [25] proposed using stationary batteries as a buffer between the grid and the charging stations, thus helping to limit the peak consumption. On the other hand, [26] explored the optimal size of battery energy storage (BES) within DCFCSs using a dynamic traffic model to minimise the DCFCSs costs.

The design criteria of DCFCSs with BES were proposed in [27] considering EV energy consumed based on the driving distance. However, in urban areas, to satisfy the load demand of the new EV models, public DCFCSs that can recharge EVs rapidly are indispensable. In our previous work, we sought to reduce DCFCSs' charging time using a modular BES within DCFCSs as a buffer to decouple the EV load from the low voltage (LV) grid [28]. In addition, the integration of DCFCSs must meet the EV demand in order to evaluate the grid-related infrastructure costs [29].

Although recent papers have recently discussed using BES with DCFCSs, more work is required to predict the DCFCSs demand given EVs' increased market penetration [2]. Additionally, the integration of the BESs within the power systems must consider the evolution of the power electronics, the new lithium-ion battery technologies [30] and the gradual reductions in the costs of BES[31].

Assuming the state-of-the-art of the public DCFCSs, this work proposes a stochastic planning method of the DCFCSs considering user behaviour and probabilistic driving patterns in order to predict EV charging demand. According to the stochastic method, a coordinated charging demand and BES charging demand are proposed with the objective of minimising peak EV load and the charging infrastructure costs. In the coordinated charging demand, the peak EV load is managed by controlling the DCFCSs in terms of power and charging duration. Instead, in the BES charging demand, an optimal BES is proposed as an alternative solution to reduce DCFCSs operational costs as well as peak EV demand. The case studies in consideration use the real data from Nordhavn Project in Copenhagen [32] such as the electrical grid, BES and the DCFCSs. In addition, the proposed stochastic planning method is formulated as a multi-objective optimisation problem based on EV charging demand. The two objectives are, first, to minimise the DCFCSs' installation and operation costs and, second, to minimise the BES systems' size.

In conclusion, the main contributions of this paper are:

- To propose a stochastic planning method to analyse the expected charging demand from the DCFCSs according to different properties and probabilistic driving patterns.
- To propose a method to determine an optimal coordinated charging demand to avoid the DCFCSs peak load in order to minimise the grid installation costs by controlling the DCFCSs.
- To propose a method to determine optimal storage charging demand to avoid the DCFCSs peak load in order to minimise the grid installation costs by integrating BES within the power systems.
- To propose a cost-benefit analysis (CBA) to evaluate the financial feasibility of BES within the power systems by considering the DCFCS costs, grid connection costs and battery life cycle cost.

This work comprises an analysis the of DCFCSs' impacts of in a realistic case study in Copenhagen grid.

The paper is organised as follows. The method used to calculate the EV demand is introduced in Section 2, and the models for the stochastic method used in determining the EV loads are described in Section 3. The optimisation problems are introduced in Sections 4, 5, 6. The results are presented in Section 7 and the conclusions in Section 8.

2. EV charging modes

The IEC 61851 describes the "electric vehicle conductive charging system," and the four charging modes. The charging modes are classified as Mode 1, 2, 3 and 4 [33]. These charging modes affect the charging power during the entire EV-charging process. The EV charing poprcess depends on the type of EV battery and on the battery-management system (BMS). Modes 1, 2 and 3 are designed to charge EVs in alternating current (AC) and the mode 4 in direct current (DC).

At the moment, the power delivered in AC is between 3kW and 43kW, and it is mainly used at home, offices or for slow public charging stations. The DC method (Mode 4) is designed only for public charging stations; it allows for charging in a short period of time. Mode 4 is implemented for off-board chargers. IEC 61851 (parts, 23 – 24) and IEC15118 provide the general requirements for the control of communication between DCFCSs and an EVs [33]. In addition, IEC15118 provides guidance on how EVs can provide power to the grid, as well as services such as voltage support and frequency regulation [34]. The evolution of power electronics, including new control interfaces and EV batteries, will play an important role in the development of competitive EVs. Table 1 summarises the main charging modes' characteristics and power levels according to IEC 61851 and IEC 62196 [33]-[35].

Table 1. *Charging modes according to IEC61851* [33]

EV50[kWh] 20% SoC	*Mode 1*	*Mode 2*	*Mode 3*	*Mode 4*	*Mode 4*	*Mode 4*
P_c [kW]	3.5	11	22	50	150	300
$t_{1\_SoC\ 80\%}$	9.15h	2.8h	1.5h	38min	12.6min	6.3min
$t_{2\_SoC\ 100\%}$	13.7h	4.3h	2.15h	1.28h	25.2min	12.7min
t_1 [km]	368	368	368	368	368	368
t_2 [km]	500	500	500	500	500	500

Recently, to reduce the charging times, many companies have started to develop DCFCSs with power ranging from 150kW to 300kW at 800V considering the socket-outlets in combined charging systems (CCSs) [30]. These new DCFCSs require a strong grid infrastructure, which carries a high investment cost. These large installed capacities also require a dedicated connection to the medium-voltage (MV) grid, including an appropriate transformer. The transformer has high economic costs and space restrictions, especially if the installation takes place in the cities. In this paper, it is assumed the EVs will be charged using Mode 4 at public charging stations in and around the Copenhagen metropolitan area. Fig. 1, shows the EV charging profile in Mode 4 tested in our laboratory [36]. In particular, Fig. 1 shows the EV charging profile in Mode 4 tested with a charger of 50kW (ABB t53) [37]. The car under consideration is a BMW i3 with 33kWh and 18% SoC.

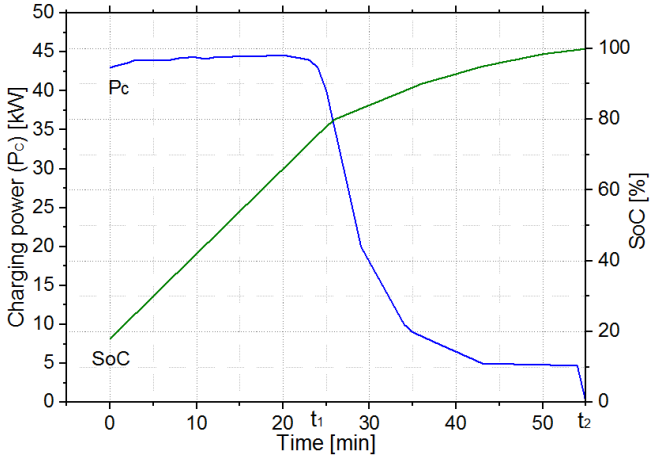

Fig. 1. *ABB EV charging profile of 50kW in DC*

The charging profile in Mode 4 can be mathematically expressed as:

$$P(t)=\begin{cases} P_C, & 0<t\le t_1 \\ P_C\cdot e^{-\frac{t}{\tau}}, & t_1<t\le t_2 \\ Pc=0, & t=t_2 \end{cases} \quad (1)$$

where *P(t) is* the charging rate at time *t, P_c* is the charging power according to charging mode in DC, τ is the charging time, t_1 represents the charging time from 18% to 80% SoC, and t_2 represents the charging time from 80% to100% SoC as shown in Fig. 1.

3. Stochastic method for EV charging demand

The EV charging demand is calculated using the charging characteristics in DC, the arrival charging time and the SoC. The SoC depends on the travel usage and can be considered a random variable related to the travel distance. According to the Danish National Transport Survey (DNTS) the average daily travel distance in Denmark is 40.1km, comprising three trips and slightly under 1 hour of travel per day. The probability distribution of the distances is shown in Fig. 2 [38] and is expressed as a lognormal type, with zero probability of a negative distance and an extension to infinity for the positive distance [39]. The probability density function (PDF) of the traditional vehicle travel distance is expressed as:

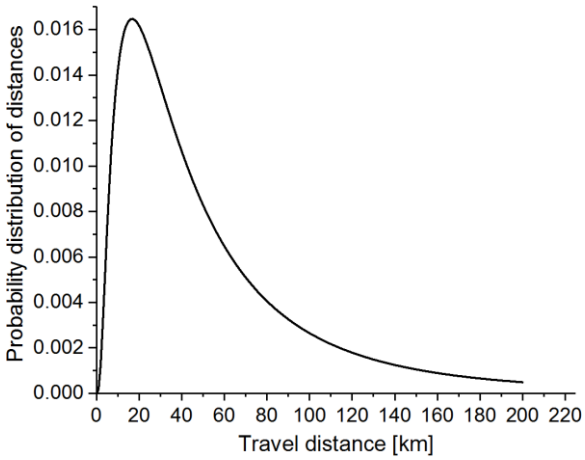

Fig. 2. *Probability of travel distance in Denmark*

$$f(d,\mu_d,\sigma_d)=\frac{1}{d\sigma_d\sqrt{2\pi}}e^{\frac{-(l_n\cdot d-\mu_d)^2}{2\sigma_d^2}},\ d>0 \quad (2)$$

μ_d and σ_d are the l_n mean and the standard deviation of the mentioned normal distribution, respectively. The travel distance in Denmark, as shown in Fig. 2 has $\mu = 3.6913$ $\sigma = 0.9361$. Since the new EVs can reach more than 400km, the probability distribution of daily travel distance for an EV is assumed to be the same as for a traditional vehicle. The future EV range will be 350-650 km for EVs with typical lithium-ion batteries of 40, 50 or 60kWh. In this case study, we use the mean values of 50kWh and 500km as shown in Table 1. The EV energy demand (EV_D) after one-day of travel can be calculated as shown in equation (3) considering a driving distance *d* of 40.1 km (2).

$$EV_D=(d\cdot V_{ec}\cdot)\cdot\frac{1}{\eta_c} \quad (3)$$

Instead, η_c represents the efficiency of the DCFCS, and V_{ec} is the vehicle's energy consumption. The energy consumption is based on the driving pattern, which changes according to the EV's performance. The current EVs' consumption vary between 0.1 and 0.2 kWh/km [28] and this paper considers V_{ec} of 0.15kWh/km. According to the daily travel distance, the SoC after one day can be calculated as:

$$SoC_0 = SoC_1 - \frac{d}{d_{\max}}, \qquad 0 < d < d_{\max} \tag{4}$$

where SoC_0 is the residual battery capacity after one day, SoC_1 is dimensionless with value 1, d is the daily travel distance of the EVs and d_{max} is the maximum range of the EVs. Assuming that SoC_0 drops linearly with the travel distance d, the PDF can be calculated by substituting equation (4) into equation (2) and changing variable form d to SoC. After one-day travel distance, the SoC based on PDF is obtained as:

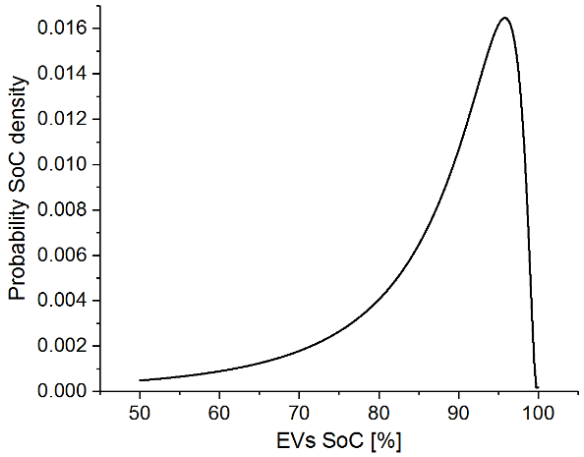

Fig. 3. *Probability density of EVs' SoC after one-day of travel*

$$f(SoC_0, \mu_d, \sigma_d) = \frac{1}{(SoC_1 - SoC_0) d_{\max} \sigma_d \sqrt{2\pi}} e^{\frac{-\left[(l_n \cdot (SoC_1 - SoC_0) + l_n \cdot (d_{\max}) - \mu_d)\right]^2}{2\sigma^2}} \tag{5}$$

Fig. 3 shows the probability density of the EVs' SoC calculated in equation (5), after one day of travel. The daily distance and the probability density of SoC are based on the two stochastic variables calculated in equations (2) and (5). The SoC after an amount of days d_n can be calculated as:

$$SoC_n = SoC_1 - \frac{d_n}{d_{\max}} \tag{6}$$

Where SoC_n is the residual battery capacity after a number of days, the SoC_1 is dimensionless with value 1.

3.1. Prediction of the EV charging demand

To predict the EVs' charging-start times several factors need to be analysed carefully including user behaviour, the daily travel distance and the home or work location of the EV users. People in the metropolitan areas will need to charge their EVs at public charging stations because most of them live and work within shared buildings. However, outside metropolitan areas, people will prefer to charge at work or at home [39]. In this paper, the start charging time of EVs is calculated by analysing internal combustion engine (ICE) vehicles and their refuelling behaviour at the petrol stations. In order to determine the EVs' charging-start time, six months of data from four petrol stations have been collected and analysed [40]. Once the data are collected the mean and the standard deviation from petrol stations can be defined. Fig. 4 shows the refuelling-time distribution of four petrol stations in Copenhagen.

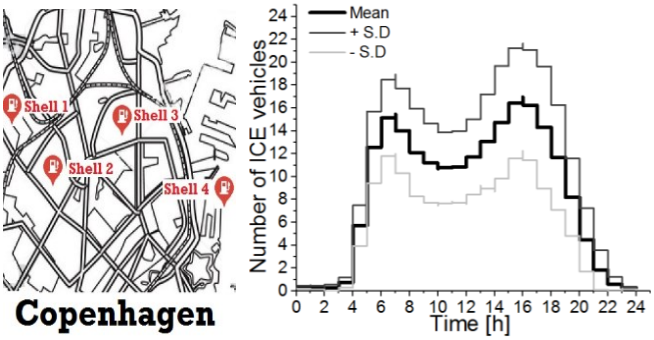

Fig. 4. *Petrol stations: number of ICE vehicles every hour*

The mean and standard deviation (SD) are calculated according to the normal distribution:

$$f(t_{st}, \mu_{st}, \sigma_{st}) = \frac{1}{\sigma_{st}\sqrt{2\pi}} e^{\frac{-(t_{st} - \mu_{st})^2}{2\sigma_{st}^2}} \tag{7}$$

t_{st} is the observation hour during the day at the time t. μ_{st} and σ_{st} are the mean and the standard deviation, respectively, of ICE vehicles sampled every hour at the four petrol stations. Fig. 5 shows PDF according to t_{st} at 7 AM, 8 AM 4 PM and 5 PM with their mean and the standard deviation.

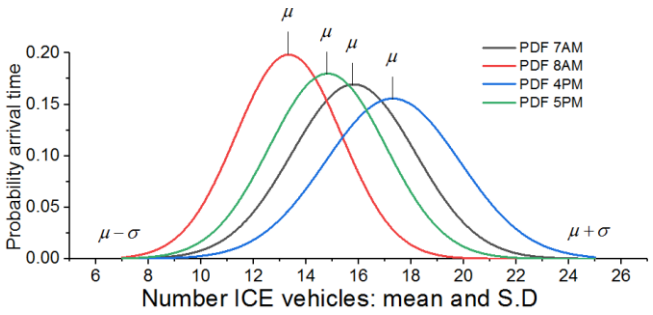

Fig. 5. *Normal distribution of vehicles at the petrol stations*

In this case, study, because new EVs have ranges of 500 km or more, we assume that the daily travel distance of an EV and the number of trips per day are the same as those of a traditional vehicle. According to this evaluation, we can define the correlation between two dependent variables: the arrival time of traditional vehicles at gas stations versus the EVs' arrival time at the charging stations. To convert the refuelling-time distribution into EVs' charging-start times, two correction factors need to be considered: first, the range in km of ICE vehicles (ICE_r) versus the range of EVs in km (EV_r), and second, the EV market penetration (EV_{mp}) in Denmark. Therefore, μ_{st} and its σ_{st} calculated in (7) need to be

converted according to EV_{mp} expressed in [%] and the EV_r in Denmark [2].

$$\mu_{ev}(t) = (\mu_{st}(t) \pm \sigma(t)) \cdot \frac{ICE_r}{EV_r} \cdot \frac{EV_{mp}}{100}, \forall t \quad (8)$$

$\mu_{ev}(t)$ is the mean number of EVs at the tth hour at the public charging stations, $\mu_{st}(t)$ is the mean number of ICE vehicles at the tth hour at the petrol stations considering $\sigma_{st}(t)$ with a confidence interval of 95%. In Copenhagen $ICEr$ vehicles have a mean driving range of 710km and the mean of EVr range in 2020-2025 will be 500km [41]. Since the EVs range is lower than $ICEr$ vehicles range, the charging frequency of EVs at the DCFCSs will be higher than the frequency of refuelling at the current petrol stations. Therefore, $ICEr/EVr$ defines the correlation between refuelling frequency of ICEr vehicles and the EVs charging frequency. According to (8), Fig. 6 shows the estimated EV arrival time at the fast charging stations around the Copenhagen metropolitan area for EV market penetrations ranging from 5% to 50% [2].

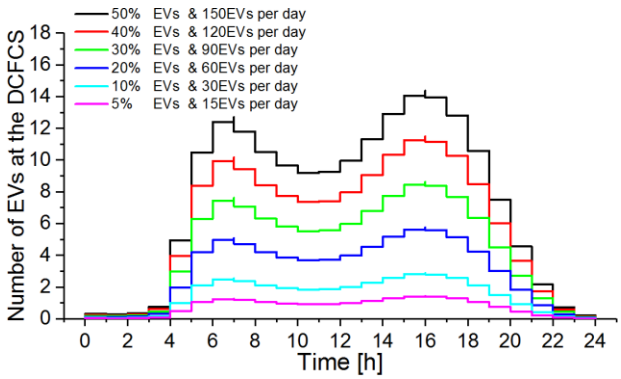

Fig. 6. *Number of EVs per hour at DCFCSs*

Therefore, the power demand of EVs can be calculated as:

$$P_{tcl}(t) = \mu_{ev}(t) \cdot P_{dc}(t) \cdot n_{dc}, \forall t \quad (9)$$

$P_{tcl}(t)$ is the total charging load at time t and P_{dc} is the DCFCSs' power based on the number of charging spots and their efficiency η_{dc}. The charging time of EVs is distributed with a random function every hour across the public DCFCSs. However, the charging duration depends on the EVs' initial SoC and on the DCFCSs' power.

4. EV charging demand methodology

In this section, large-scale EVs are assumed to be incorporated within the power systems of the Copenhagen Nordhavn area [32]. The proposed stochastic planning method is presented to evaluate the public DCFCSs' demand and grid impact. In this paper, three different DCFCS layouts are analysed: uncontrolled charging demand, controlled charging demand and storage charging demand.

4.1. Uncontrolled charging demand

In the uncontrolled charging scenario, each EV will start charging when it reaches a low level of SoC, especially when SoC_n after a number of trips cannot satisfy the next travel distance SoC_{nt} programmed from the drivers.

$$SoC_n < SoC_{nt} \quad (10)$$

The SoC_{nt} can be calculated according to the daily travel distance calculated in equation (2), and it can be assumed to be equal to around 10% SoC. In addition, for the uncontrolled charging demand, both the grid's power conditions, $P_g(t)$, and the available power from the transformer must satisfy the EV load demand.

$$P_g(t) \leq P_{tcl}(t) \quad (11)$$

The number of charging spots can be calculated based on the maximum daily EV demand, which can be calculated using equations (3), (6), and (10), after a number of trips as:

$$EV_D = (\mu_{evt} \cdot SoC_{nt} \cdot d_{\max} \cdot V_{ec}) \cdot \frac{1}{\eta_c} \quad (12)$$

μ_{evt} is the number of EVs per day, which is calculated as shown in Fig. 6; in addition, V_{ec} is the vehicle energy consumption, which is considered 0.15kWh/km for a charging efficiency η_c of 95% [28]. Table 2 shows various daily EV demands and the minimum grid power required to support EV demands as shown in equation (12).

Table 2. *Charging spots based on EVs demand*

EV Market [%]	*Number EVs per day*	*EV demand EV_D[kWh]*	*Grid power P_{gr}[kW]*	*Number DCFCS 50kW*	*Number DCFCS 150kW*
5%	15	896	72.2	2	1
10%	20	1792.0	144.3	3	1
20%	60	3583.9	288.6	6	2
30%	90	5375.9	433.0	9	3
40%	120	7167.9	577.3	12	4
50%	150	8959.9	721.6	15	5

$$P_{gr} = \frac{EV_D[kWh]}{\mu_{evp}[h]} \quad (13)$$

P_{gr} represents the minimum required grid power and μ_{evp} represents the maximum EV demand during the congested peak hour of the day as shown in Fig. 6. The number of charging spots and their power levels will determine the maximum power required from the grid. Once the daily EV demand is defined, the network parameters and the number of charging spots can be modeled as well as a CBA can be performed based on the EV demand.

4.2. Coordinated charging demand

In the coordinated charging scenario, the DCFCSs are controllable. The primary objective is to minimise the peak-load when the DCFCSs demand exceeds the grid power. According to the IEC15118 [34], we define three controllable charging loads. The first involves setting the DCFCSs' nominal power to a predefined value. The second involves setting the charging duration using the DCFCSs' nominal power. The third involves setting the nominal power and charging duration to specified values. The three control settings can be expressed as:

$$P^c_{tcl}(t) = \mu_{ev}(t) \cdot (P_{dc,i} \cdot \alpha(t) \cdot \beta(t) \cdot \gamma(t)) \cdot n_{dc}, \forall t \quad (14)$$

where $P^{c}_{tcl}(t)$ is the controlled load demand during the day by using the three control settings parameters. α is the DCFCS charging power setting to a predefined value that can vary from 0 to 1. β is the charging duration of the DCFCSs expressed in minutes. Instead, γ includes α and β. In addition, α, β and γ are three independent parameters. The selected parameters define the communication protocols and the controllability modes between the DCFCS and the EV according to international standard IEC15118 [34]. In our case, the coordinated charging mode of each DCFCS is controllable by γ. Using γ avoids the congested peak hours during the workday by reducing the DCFCSs' nominal power and charging duration. The objective in equation (15) is to provide as much energy as possible to the users according to the grid conditions $P_g(t)$ at the time t. The controlled load can be expressed as:

$$\begin{cases} \max\left(P^{c}_{tcl}(t)\right) \\ if: P^{c}_{tcl}(t) > P_g(t) \\ set\ \gamma\ with\ P^{c}_{tcl}(t) = P_g(t) \\ if: P^{c}_{tcl}(t) < P_g(t) \\ set\ \gamma = 1 \end{cases} \tag{15}$$

Therefore, the nominal DCFCSs power can exceed the available power of the transformer as long as γ is used to set the DCFCSs power.

4.3. Storage charging demand

In this section, an optimal PS management is proposed to minimise the EV load during the congestion hours by using BES as a stationary application. The introduction of the BES within the DCFCs helps to minimise the DCFCSs' operation costs and reduce the charging time during the congestion hours. The cost reduction of the lithium-ion batteries is an important parameter, which must be taken into account. This represents an opportunity to integrate the EVs' penetration and charging systems into the power systems. The BES systems have been estimated to decrease in price by 8% annually [31]. DCFCSs, in combination the BES, can thus represent a smart way of minimising grid-reinforcement costs and meeting EV demand during peak hours. In this case study, the controllability mode is not used, and the EVs peak demand will be supported by the BES. Storage charging demand must include the system's overall power balance over a specified time:

$$\begin{cases} P_g(t) = P_{tcl}(t) - \dfrac{P_{b,dis}(t)}{\eta_{dis}} & , if\ \text{discharging} \\ P_g(t) = P_{tcl}(t) + P_{b,ch}(t)\cdot\eta_{ch}, & if\ \text{charging} \end{cases} \tag{16}$$

$P_b(t)$ is the power given or absorbed from the BES, η_{dis} and η_{ch} are the BES's converter efficiency which is 95% during the discharging and charging processes, respectively. The objective function is used to minimise the EV energy peak demand by using the minimum BESs $E_b(t)$ within the DCFCSs as described in the following equations:

$$\begin{cases} \min\left(E_b(t)\right) \\ E_b(t) = E_b(t_0) - \sum_{t=0}^{T}\left(E_{tcl}(t) - E_g(t)\right) + \sum_{t=0}^{T}\left(E_g(t) - E_{tcl}(t)\right) \\ if: E_{tcl}(t) > E_g(t)\ , \text{discharging } BES \\ if: E_{tcl}(t) < E_g(t)\ , \text{charging } BES \end{cases} \tag{17}$$

$E_g(t)$ is the grid energy, $E_b(t_0)$ is the BES at the time t_0, $E_{tcl}(t)$ is the energy required from the DCFCSs during the discharging and charging processes according to available energy $E_g(t)$. During the EVs charging demand, the BES operates in parallel with the DCFCSs, and the PS is provided during the congestion hours due to the high EV demand. The BES charging power is limited by the available grid power $P_g(t)$ at the time t. The discharging power is defined by the converter's power and the difference between the grid and the DCFCSs power (16). The BES is calculated based on equations (16) and (17). Once the BES size is defined, a CBA can be implemented in order to evaluate the financial feasibility of BES within the DCFCSs by considering the installation costs, grid connection and battery life cycle cost.

5. Results of the EVs charging demand

This case study consideres the future EVs demand in Copenhagen, which could vary from 15 to 300 EVs per day for each charging station. As shown in Table 2, the minimum power required from the grid depends on the daily EV demand and on the EVs' market penetration. To analyse the EV demand, three scenarios have been considered: uncontrolled charging demand, coordinated charging demand, storage charging demand. All scenarios consider chargers of 150kW in DC. The 150kW charging profiles are obtained considering the performed tests in our laboratory with chargers of 50kW in DC as shown in Fig. 1 [36]. In addition, based on the performed tests, the 150kW charging profile is assumed to follow the same trend of the 50kW charger as described in equation (1). To generate the 150kW-DCFCSs' load demand simulations are carried out by using MATLAB/Simulink for the given mean and standard deviation functions (7), (8). The distribution functions of those random variables can be obtained from the equations calculated in Section 3 and 4.

5.1. Results for uncontrolled charging demand

This scenario considers the daily EV demand from 15 to 150 EVs in Nordhavn-Copenhagen area as shown in Table 2. Various charging configurations can be utilised to support the EV demand. As shown in Table 2, the minimum grid power required to support the EVs demand varies according to the EVs demand. In all scenarios chargers of 150kW are considered. Fig. 7 shows the results from five DCFCSs, where all the input parameters are assumed to follow the stochastic demand model calculated in Section 3 and 4. The DCFCSs load profile is one of the most critical parameters obtained from the stochastic model. It shows the daily pulsating load profiles of the EVs charging demand on the grid side according to equations (9) and, (11). The case study considers 50 % EV market penetration and five chargers of 150kW, as shown in Fig. 7.

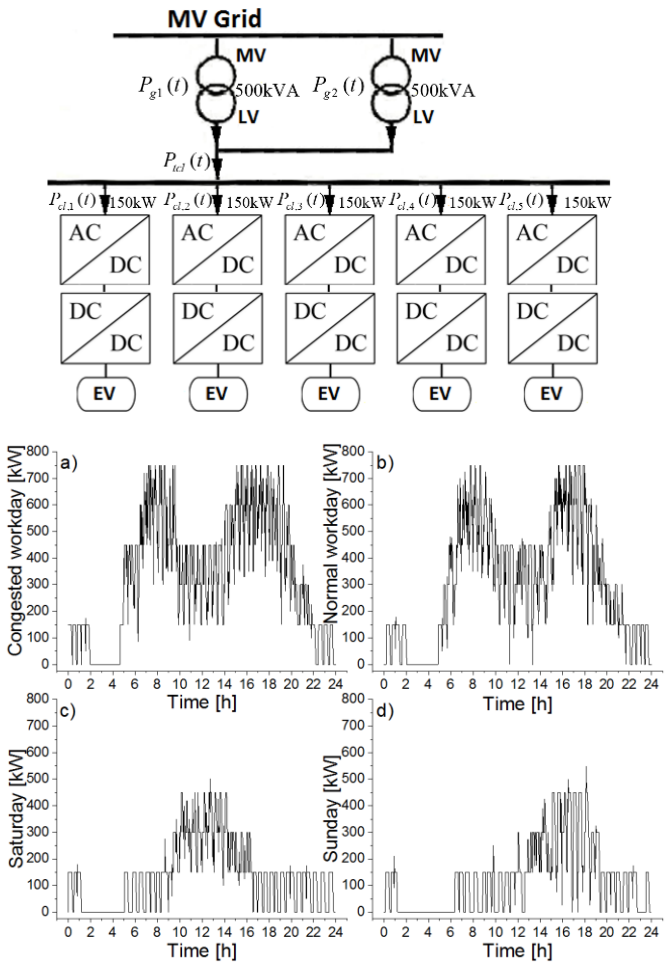

Fig. 7. *DCFCSs load demand for: a) a congested workday 150EVs, b) a normal workday 140EVs, c) Saturday 90EVs, d) Sunday 80EVs*

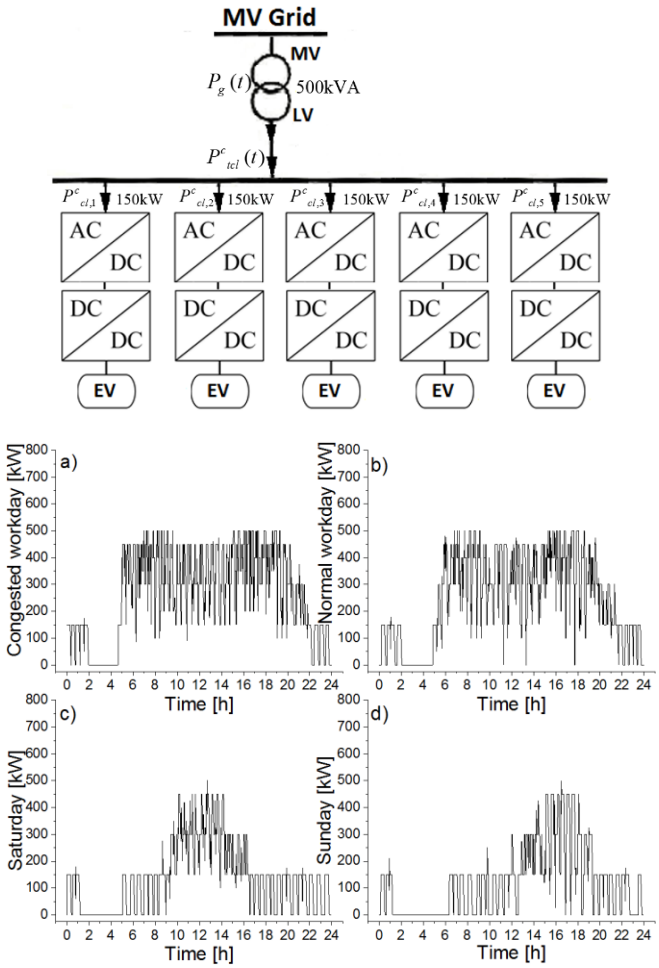

Fig. 8. *DCFCSs load demand for: a) congested workday 150EVs, b)a normal workday 140EVs, c) Saturday 90EVs, d) Sunday 80EVs*

Fig. 7 shows five DCFCSs of 150kW supplied by two transformers of 500kVA. The EV demand is considered for a congested workday, a normal day, a Saturday, and a Sunday. According to Table 2, in this scenario, two transformers can serve150 EVs and 140 EVs during the congestion and the normal workdays, respectively. For this grid configuration, high investment costs are required to reinforce the grid by adding a new transformer, especially when the EVs demand will increase over the years. Therefore, as shown in Fig.7, in addition to the initial investment, which includes one MV transformer and two or three DCFCSs of 150kW over the next 10 years, an additional MV transformer will be required to support the growing number of EVs. The new MV transformer requires a new investment cost which includes new dedicated LV and MV lines, switchboards as well as the installation costs [28]. In the next section, a CBA is performed according to the EV demand.

5.2. Results for coordinated charging demand

In the optimal coordinated strategy, the primary objectives are to minimise the peak-load demand and to reduce the grid-reinforcement costs. In the coordinated charging mode, each DCFCS is controllable using α, β and γ according to equations (14) and (15). In this case study, γ is used to control DCFCSs during the peak hours by reducing the nominal DCFCSs power and the charging duration, as shown in Fig. 8.

Fig. 8 shows five DCFCSs of 150kW and the EV demand during a congested workday, a normal workday, a Saturday, and a Sunday with α =100kW and β =15min. The controllability mode can (as shown in this case) be used as a multifunctional grid-utility with the main objective of minimising the EV load demand during peak hours using an optimal coordinated strategy of γ (15). Using γ reduces the grid-reinforcement costs and costs of the new transformer's substation. Nevertheless, the controllability mode must meet certain criteria, as it also has several different disadvantages. For example, reducing the power and charging duration can affect the users' comfort because the EVs are partially charged during the congestion. In addition, the controllability mode of the charging stations is a trade-off between grid constraints and the DCFCSs' needs. Therefore, for this grid configuration, a CBA is not required because the costs and benefits are similar to Section 5.1.

5.3. Results for storage charging demand

The storage charging demand reduces the DCFCS load during congested workdays, when the EV demand is high. As shown in Fig. 7, the EV load demand has a high power fluctuation especially in the morning and the late evening. The introduction of BESs within the DCFCSs helps to reduce the charging-infrastructure costs and the negative impacts of congestion. The BES stores electrical energy during off-peak hours and returns the stored energy to the grid during peak hours as described in equation (16).

In the optimal storage strategy, the primary objectives are to minimise the peak demand and to reduce grid-reinforcement costs. Consequently, an optimal BES size is determined to support the EV demand during a congested workday and a typical workday. According to Table 2, the charging-storage method considers the daily demand from 100 to 150 EVs for which either grid reinforcement or BES is required. As shown in Table 2, the minimum charging power is 600kW to support the EV demand from 100 to 130 EVs/day, and with a demand from 140 to 150 EVs/day, the minimum charging power is 750kW. Thus, four or five chargers of 150kW are required for a normal and a congested workday. In this case study, with demand from 100 to 150 EVs/day the grid power is fixed at 500kW, and the remaining energy will be provided by the BES which is connected in parallel as shown in Fig. 9. The EV load can be obtained from the equations calculated in Section 3 and 4. Fig. 9 shows five DCFCSs of 150kW and an EV demand during a congested workday. The storage-charging interface plays an important role during the congested hours, and it can be used as a multifunctional grid-utility with the primary objective of minimising the peak EV demand through the optimal coordination of BES.

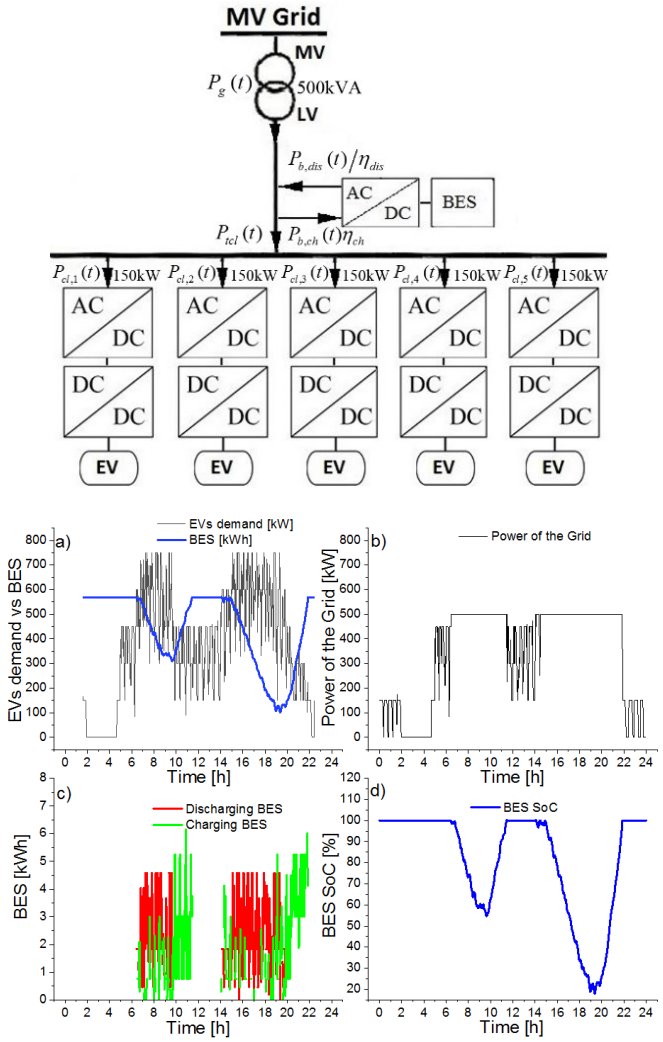

Fig. 9. *DCFCSs load for150 EVs: a) EV demand and BES in kWh, b) required grid power, c) BES charging and discharging process, d) BES SoC during the EV demand*

As shown in Fig. 9, the EV load demand fluctuates significantly, especially in the morning and the late evening. At this stage, the BES helps to prevent the grid reinforcement by providing power to the grid during peak hours. The optimal BES size varies as a function of the daily EVs demand, as shown in Table 3. In addition, the integration of BESs within the power systems is a trade-off between the grid reinforcement costs and the BES investment cost. Table 2 shows EVs daily demand from 15 to 90 EVs where the grid reinforcement is not required. However, from 100 to 150 EVs grid reinforcement is required to support the demand. Alternatively, as shown in Table 3 the storage charging demand can prevent the grid upgrade by using different BESs as grid reinforcement.

Table 3. *Storage and charging strategy*

Number EVs per day	*Grid power [kW]*	*Power DCFCSs [kW]*	*Overload grid [%]*	*Overload time [h]*	*BES [kWh] E_b*
15	500	150	0	0	0
20	500	150	0	0	0
60	500	300	0	0	0
90	500	450	0	0	0
100	500	600	20	1.04	18.2
110	500	600	20	1.27	23.5
120	500	600	20	2.13	28.17
130	500	600	20	3.18	31.12
140	500	750	50	5.15	437
150	500	750	50	7.44	586

The BES size is calculated according to equation (17). Based on Table 3 a CBA is analysed as a function of various BES size to evaluate the financial feasibility of BES within the DCFCSs by considering daily demands from 15 to 150EVs.

6. Cost-benefit analysis methodology

This section two cases of grid reinforcement are considered. A CBA approach is used to compare the profitability of the DCFCSs investment within power systems considering different EVs charged per day.

In the first case, Case A uses the BESs as stationary application during the congestion hours to support increasing EV demand over the years as shown in Table 4 and Section 5.3. In this case, the BES operates as PS in parallel with the grid. In the second case, Case B adopts grid reinforcement by using a new MV transformer to sustain the increasing EV demand over the years as shown in Table 4 and Section 5.1.

Table 4.*CBA of the case A and B*

Number of EVs per day	*Number of DCFCSs 150kW*	*Case A grid power [kVA]*	*Case B grid power [kVA]*
15	1	500	500
20	1	500	500
60	2	500	500
90	3	500	500
100	4	500+BES	1000
110	4	500+BES	1000
120	4	500+BES	1000
130	4	500+BES	1000
140	5	500+BES	1000
150	5	500+BES	1000

In both cases, at the beginning, reinforcement of the MV grid is required with a transformer of 500kVA as shown in Table 4. Since the EVs demand will increase during the years [2], extra chargers will be required to sustain the EVs demand. As shown in Table 4, 500kVA is the minimum grid power required to support the demand up to 90 EVs/day. However, if the EV demand increases over the years from 100 to 150 EVs per day, new chargers in DC, as well as a new transformer of 500kVA must be installed. The main objective of the CBA is to evaluate the economic performance of Case A versus Case B. In particular, the financial performance of Case A, which must take into account the BES costs and the lifetime versus a traditional grid upgrade.

The key parameters of the CBA are listed below.

The payback period *(PBP)* is the amount of time necessary to recover the investment, which can be calculated as follows [42]:

$$PBP = \frac{C_t}{B_t} \tag{18}$$

C_t represents the cost of the investment, and B_t is the annual benefit or revenue per year during the investment period T.

Net present value *(NPV)* is the present value of cash inflows and the present value of cash outflows [42]:

$$NPV = \sum_{t=1}^{T} \frac{B_t}{(1+r)^t} - \sum_{t=1}^{T} \frac{C_t}{(1+r)^t} - C_0 \tag{19}$$

r is the discount rate or interest, and C_0 is the initial investment cost.

Instead, the method used to evaluate the economic performance of one or more investments is the benefit-cost ratio *(B/C)*, which can be expressed as follows [42]:

$$B/C = \frac{NPV\,(\text{Benefits})}{NPV\,(\text{Costs})} = \frac{\sum_{t=1}^{T} \frac{B_t}{(1+r)^t}}{\sum_{t=1}^{T} \frac{C_t}{(1+r)^t} + C_0} \tag{20}$$

The costs and revenues are calculated for the two cases under consideration: the Case A – DCFCSs with BES and Case B – DCFCSs considering a new connection to the MV grid.

6.1. Case A cost and revenue

In Case A, the annual costs and benefits associated with adding BES to the charging stations can be calculated using the infrastructure costs and as benefits the consumption of electricity from the EV users.

The total annual costs of Case A ($C_{t,A}$) are calculated as:

$$C_{t,A} = C_A + C_I + C_{OM} \tag{21}$$

C_I is the installation cost, and C_{OM} is the operation and maintenance cost. Instead, C_A includes component costs, as the chargers cost C_C, and the batteries cost considering replacement during the investment life t (22).

$$C_A = \sum_{t=1}^{T} BES_{D,t} \cdot C_{BES,t} + C_C \tag{22}$$

BES_D is the BES degradation life per year, C_{BES} represents the BES costs per kWh considering replacement costs during investment life T. The BES_D can be calculated as:

$$\begin{cases} E_D(t) = \int_0^t |P_b(t)|\,dt \\ K_{PYD} = \dfrac{E_D \cdot \Delta_{Te}^{-1}}{2 \cdot E_b} \\ BES_D = \dfrac{K_{PYD}}{K_{BES}} \end{cases} \tag{23}$$

$E_D\,(t)$ represents the enegry consumed at time t. Instead, $P_b\,(t)$ is the power provided from the BES during the PS process. In addition, K_{PYD} considers the number of cycles utilised during a year. BES_D is the BES degradation per year under at a predefined variable work temperature Δ_{Te} =0,9814 [43]. K_{BES} are the number of cycles given by the manufacturers.

The total annual benefits or revenue for Case A ($B_{t,A}$) can be calculated as:

$$B_{t,A} = (E \cdot Ce) \cdot t_t \tag{24}$$

where E is the daily energy consumed as a function of the EV demand, which is calculated in (12). C_e is the cost of electricity paid by the EV users and t_t is the total time in a year.

6.2. Case B cost and revenue

In the Case B the annual costs and benefits associated to grid upgrade are calculated considering the infrastructure costs such as new lines and a transformer of 500 kVA as well as the installation and DCFCS costs [28]. Instead, the benefits are calculated considering the consumption of electricity from EVs as shown in (24).

The total annual costs for Case B ($C_{t,B}$) are calculated as:

$$C_{t,B} = C_B + C_I + C_{OM} \tag{25}$$

where C_B is the component cost, which includes the costs of the chargers, lines, and transformer. The total annual revenue for Case B ($B_{t,B}$) can be calculated as shown in (24).

7. Cost-benefit analysis results

In this section, two separate layouts to connect the charging systems within the power systems are considered. Case A considers a CBA by using BES as stationary application during the congestion hours to support the increasing EV demand over the years as shown in Fig. 10. In this case, the BES provides PS only during the congestion hours. Instead, Case B considers a CBA by using a new grid reinforcement to MV grid to sustain the increasing EV demand over the years. In both cases, at the beginning, a grid reinforcement is required with a transformer of 500kVA. A flowchart model is proposed for each scenario based on the same EV demand per day as shown in Fig. 10.

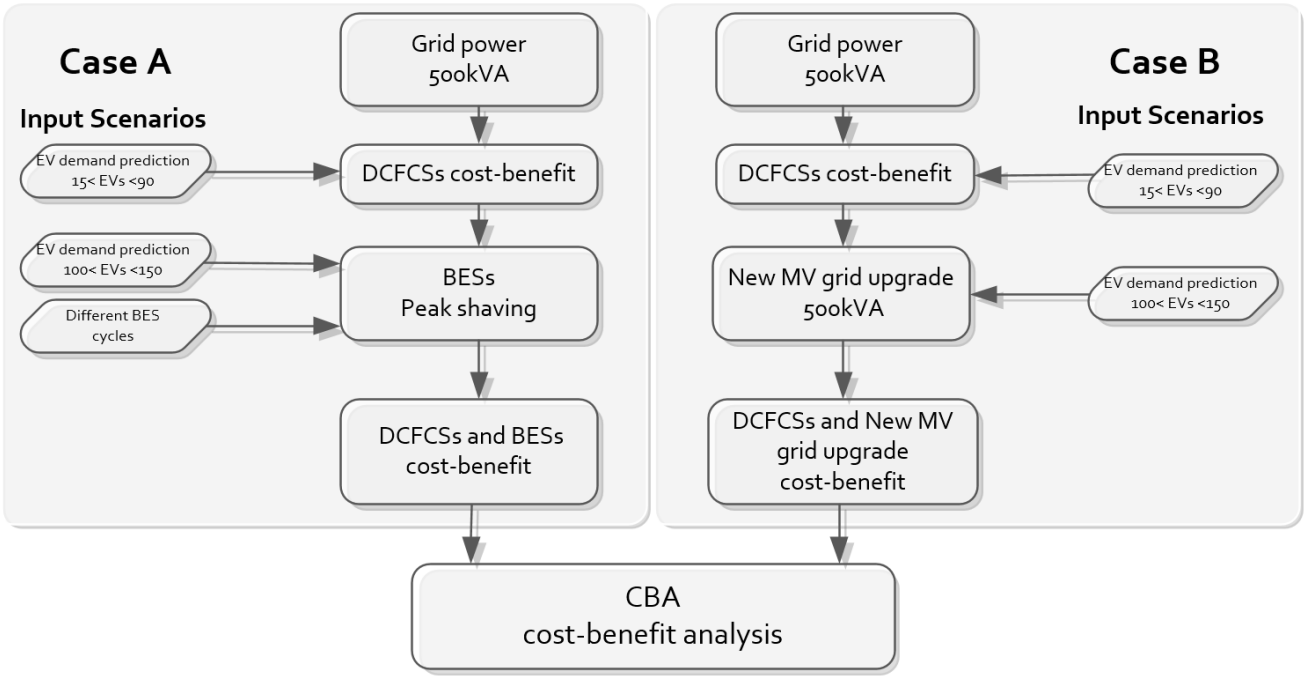

Fig. 10. *Case A grid integration of BES and DCFCSs and Case B standard integration of DCFCSs with a MV grid upgrade*

7.1. Case A: CBA of DCFCSs considering BES as peak shaving

The primary objective of this CBA is to estimate the infrastructure costs of the Case A and costs of BES across its lifetime. The benefits and the costs of the Case A are calculated as shown in Section 6.1. It was shown that EVs demand from 15 to 90 EVs requires a minimum grid power of 500kVA as an initial investment. However, if the demand increases over the years from 100 to 150 EVs, new DCFCSs, and a new transformer of 500kVA are required to meet the increasing EV demand. To avoid new grid-reinforcement costs, the BES operates in parallel with the DCFCSs, as shown in Fig. 9. In Case A, three different lithium –ion technologies are considered, the current technology battery lithium nickel manganese cobalt oxide (NMC) with 5000 and 10000 cycles [44] and a future scenario lithium titanate oxide (LTO) battery with 25000 cycles [45]. The number of EVs charged per day is used to calculate the total annual benefits $B_{t,A}$ calculated in equation (24) based on the annual energy consumed from users. Instead, $C_{t,A}$ is calculated based on the equations (21) and (22). The equations consider the investment costs including, the component costs: DCFCS costs, BES replacement costs (22), converter costs and the installation costs. Once $C_{t,B}$ and $B_{t,A}$ are defined, *PBP* equation (18), *NPV* equation (19), and *B/C* ratio equation (20) can be calculated as shown in the proposed Section 6 using the CBA methodology.

7.2. Case B: CBA of DCFCSs considering MV grid upgrade

The primary objective of this CBA is to establish the infrastructure costs of Case B in order to justify a standard investment of MV grid reinforcement. In Case B when EV demand increases from 100 to 150 EVs, new DCFCSs, as well as a new transformer of 500kVA are required to meet the increasing EV demand as shown in Fig. 7. The benefits and the costs of Case B are calculated in Section 6.2. The number of EVs charged per day is used to calculate the total annual benefits $B_{t,B}$, as shown in equation (24). Instead, $C_{t,B}$ equation (25) is the investment costs including grid reinforcement costs. The infrastructure costs of Case B are DCFCS costs, the costs of the new dedicated lines for both the LV and MV grids, the cost of the new transformer of 500 kVA as well as the installation costs. Once $C_{t,B}$ and $B_{t,B}$ are defined, *PBP* equation (18), *NPV* equation (19), and *B/C* ratio equation (20) can be calculated as shown in Section 6 using the CBA methodology.

7.3. Economic assessment of Case A and Case B

In this section, an economic assessment is carried out to compare the costs and benefits of Case A and Case B. The economical results of Case A and B are: the *PBP*, *NPV* and *B/C* ratio which is summarised in Fig. 11, and in Tables 6, 7, and 8. All the economic parameters used in Case A and Case B are listed in Table 5:

Table 5. *Costs and benefits of Case A and Case B*

Case A	***Costs [€]***	***Benefits***	***Case B***	***Costs [€]***	***Benefits***
DCFCS cost [37]	50000		DCFCS cost [37]	50000	
BES price €/kWh [31]	200		Component costs [28]		
EV demand: 45 kWh			EV demand: 45 kWh		
Electricity price paid by EV users [2]		0.6 €/kWh	Electricity price paid by EV users [2]		0.6 €/kWh
Discount rate (r): 8% [46]			Discount rate (r): 4% [47]		
Investment life: 20 years			Investment life:20 years		

The grid investment for the upgrade is based on a 4% discount rate [47]. However, the investment in BES can be considered riskier than that in the grid reinforcement. Therefore, the interest rate used for BES is 8% [46]. Fig. 11 compares the financial performance of Case A and Case B considering three types of batteries with different cycles. As mentioned,

Case A requires the integration of BES to support the grid when the daily EV demand exceeds 90 EVs. As shown in Fig. 11, in Case A the red and orange lines represent the current technology of lithium-ion NMC battery with 5000 and 10000 cycles respectively [44]. The blue line is the future generation of lithium-ion LTO battery with 25000 cycles [45]. Instead, in Case B, the black line shows the financial performance of using a new connection to the MV grid.

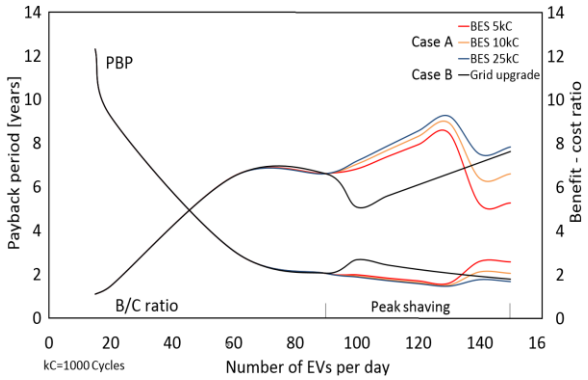

Fig. 11. *Economic comparison of the Case A PS through BES and Case B MV grid upgrade*

Tables 6 and 7 summarise the main economic assessment of the Case A, considering BES as a stationary application in parallel with the grid. Instead, Table 8 summarises the main economic assessment of Case B considering a new grid reinforcement in MV.

Table 6. *BES 10000 cycles - economic assessment: Case A*

Number EVs per day	*Grid power [kVA]*	*BES [kWh] E_b*	*Investment cost [€] C_{LA}*	*Benefits [€] B_{LA}*	*PBP [years]*	*NPV [€]*	*B/C ratio*
15	500	0	720000	58413	12.33	73858	1.10
20	500	0	720000	77885	9.24	338477	1.47
60	500	0	720000	233654	3.08	2455432	6.49
90	500	0	720000	350481	2.05	4043148	6.62
100	500	18.2	750941	389423	1.93	4541446	7.05
110	500	23.5	757120	428365	1.77	5064505	7.69
120	500	28.17	763299	467308	1.63	5587565	8.32
130	500	31.12	769478	506250	1.52	6110624	8.94
140	500	437	1157601	545192	2.12	6251740	6.40
150	500	586	1201235	584135	2.06	6737345	6.61

Table 7. *BES 25000 cycles - economic assessment: Case A*

Number EVs per day	*Grid power [kVA]*	*BES [kWh] E_b*	*Investment cost [€] C_{LA}*	*Benefits [€] B_{LA}*	*PBP [years]*	*NPV [€]*	*B/C ratio*
15	500	0	720000	58413	12.33	73858	1.10
20	500	0	720000	77885	9.24	338477	1.47
60	500	0	720000	233654	3.08	2455432	6.49
90	500	0	720000	350481	2.05	4043148	6.62
100	500	18.2	736111	389423	1.89	4556276	7.19
110	500	23.5	738582	428365	1.72	5083043	7.88
120	500	28.17	741054	467308	1.59	5609810	8.57
130	500	31.12	743526	506250	1.47	6136577	9.25
140	500	437	1000521	545192	1.77	6408821	7.51
150	500	586	1017974	584135	1.68	6920606	7.84

Table 8. *Grid upgrade economic assessment: Case B*

Number EVs per day	*Grid power [kVA]*	*Investment cost [€] C_{LB}*	*Benefits [€] B_{LB}*	*PBP [years]*	*NPV [€]*	*B/C ratio*
15	500	720000	58413	12.33	73858	1.10
20	500	720000	77885	9.24	338477	1.47
60	500	720000	233654	3.08	2455432	6.49
90	500	720000	350481	2.05	4043148	6.62
100	1000	1040000	389423	2.67	4252387	5.09
110	1000	1040000	428365	2.43	4781625	5.60
120	1000	1040000	467308	2.23	5310864	6.11
130	1000	1040000	506250	2.05	5840103	6.62
140	1000	1040000	545192	1.91	6369341	7.12
150	1000	1040000	584135	1.78	6898580	7.63

The economic assessment of Case A is subject to the life-cycle costs of the batteries. On the contrary, the assessment for Case B (classic grid reinforcement) depends on the number of EVs charged per day. Case A, as shown in Fig. 11 with a demand from 90 to 130 EVs the B/C ratio is higher than Case B. However, if the EV demand is from 140 to 150 the Case A has the B/C ratio higher than Case B as long as the number of BES cycles is higher than 25000.

8. Conclusions

In this paper, a stochastic planning method was proposed to determine the DCFCS load profile and its impact on power distribution systems. Stochastic charging profile was used exclusively to calculate the key factors of the EVs charging demand: charging start times and DCFCSs grid impact. According to the stochastic method, a DCFCSs load demand was proposed to optimise the required grid capacity of the public DCFCSs considering real data from the user behaviour including driving-distance probability and charging-time probability. Different layouts were considered within the stochastic planning method, as the coordinated charging demand and storage charging demand.

In the "coordinated charging demand", an optimisation model was adopted to minimise the DCFCSs peak-load during the congestion periods by controlling the power and charging duration. Setting strategies were implemented as a multifunctional optimisation problem with the primary objective of minimising grid-reinforcement costs.

Instead, in the "storage charging demand", an optimisation model was adopted by using BESs within DCFCSs to minimise the peak EV load and the power fluctuation during the congestion hours. BESs with different cycles were proposed to avoid the grid reinforcement costs when the DCFCSs demand exceeds the grid's capacity. In addition, the stochastic planning method was used to minimise the grid installation and operation costs as well as to limit BES size by maximising the energy demand required form DCFCSs.

An economic assessment for the proposed solution was performed, and *PBP*, *NPV* and *B/C* ratio were considered to evaluate the financial performance of a BES investment versus grid-reinforcement costs. The economic assessment of Case A was bound by the life cycle cost of the batteries. On the contrary, the costs in Case B (grid reinforcement) were linked to daily EV demand. Consequently, Case A using BES with cycles from 10000 to 25000 has higher B/C ratio than Case B as long as the daily demand is between 90 and 130 EVs. Instead, with daily demand is from 140 EVs or more the Case A has a higher B/C ratio than Case B as long as the number of BES cycles is higher than 25000.

9. References

[1] European commission:, "'mobility and transport' www.ec.europa.eu/transport, reoprt." 2018.

[2] IEA: International Energy Agency, "Nordic EV Outlook 2018," https://webstore.iea.org/nordic-ev-outlook-2018.

[3] N. Ba, A. Tabares, J. F. Franco, and M. Lavorato, "Robust Joint Expansion Planning of Electrical Distribution Systems and EV Charging Stations," *IEEE Trans. Sustain. Energy*, vol. 9, no. 2, pp. 884–894, 2018.

[4] Z. Peng and L. Hao, "Decentralized Coordination of Electric Vehicle Charging Stations for Active Power Compensation," in *2017 IEEE 86th Vehicular Technology Conference (VTC-Fall)*, 2017, pp. 1–5.

[5] K. Kasturi and M. R. Nayak, "Optimal planning of charging station for EVs with PV-BES unit in distribution system using WOA," in

Proceedings - 2017 2nd International Conference on Man and Machine Interfacing, MAMI 2017, 2018, vol. 2018–March, pp. 1–6.

[6] C. Sheppard, A. Harris, and A. Gopal, "Cost-Effective Siting of Electric Vehicle Charging Infrastructure with Agent-Based Modeling," *IEEE Trans. Transp. Electrif.*, vol. 7782, no. MARCH, pp. 1–1, 2016.

[7] S. Shojaabadi, S. Abapour, M. Abapour, and A. Nahavandi, "Optimal planning of plug-in hybrid electric vehicle charging station in distribution network considering demand response programs and uncertainties," *IET Gener. Transm. Distrib.*, vol. 10, no. 13, pp. 3330–3340, 2016.

[8] M. Neaimeh, S. D. Salisbury, G. A. Hill, P. T. Blythe, D. R. Scoffield, and J. E. Francfort, "Analysing the usage and evidencing the importance of fast chargers for the adoption of battery electric vehicles," *Energy Policy*, vol. 108, no. April, pp. 474–486, 2017.

[9] A. Gusrialdi, Z. Qu, and M. A. Simaan, "Distributed Scheduling and Cooperative Control for Charging of Electric Vehicles at Highway Service Stations," *IEEE Trans. Intell. Transp. Syst.*, vol. 18, no. 10, pp. 2713–2727, 2017.

[10] P. Grahn, "Electric Vehicle Charging Modeling, Doctoral Thesis KTH Universily, Stockholm, 2014."

[11] G. Hill, P. T. Blythe, and C. Higgins, "Deviations in Markov chain modeled electric vehicle charging patterns from real world data," *IEEE Conf. Intell. Transp. Syst. Proceedings, ITSC*, pp. 1072–1077, 2012.

[12] R. J. Bessa, M. A. Matos, F. J. Soares, and J. A. P. Lopes, "Optimized Bidding of a EV Aggregation Agent in the Electricity Market," *IEEE Trans. Smart Grid*, vol. 3, no. 1, pp. 443–452, Mar. 2012.

[13] F. J. Soares, J. A. Pecas Lopes, and P. M. Rocha Almeida, "A Monte Carlo method to evaluate electric vehicles impacts in distribution networks," in *2010 IEEE Conference on Innovative Technologies for an Efficient and Reliable Electricity Supply*, 2010, vol. 77, no. 5, pp. 365–372.

[14] S. Habib, M. M. Khan, F. Abbas, L. Sang, M. U. Shahid, and H. Tang, "A Comprehensive Study of Implemented International Standards, Technical Challenges, Impacts and Prospects for Electric Vehicles," *IEEE Access*, vol. 6, no. March, pp. 13866–13890, 2018.

[15] O. Erdinc, A. Tascikaraoglu, N. G. Paterakis, I. Dursun, M. C. Sinim, and J. P. S. Catalao, "Optimal sizing and siting of distributed generation and EV charging stations in distribution systems," *2017 IEEE PES Innov. Smart Grid Technol. Conf. Eur. ISGT-Europe 2017 - Proc.*, vol. 2018–Janua, pp. 1–6, 2018.

[16] M. R. Sarker, H. Pandžić, K. Sun, and M. A. Ortega-Vazquez, "Optimal operation of aggregated electric vehicle charging stations coupled with energy storage," *IET Gener. Transm. Distrib.*, vol. 12, no. 5, pp. 1127–1136, 2018.

[17] O. Beaude, S. Lasaulce, M. Hennebel, and J. Daafouz, "Minimizing the impact of EV charging on the electricity distribution network," *2015 Eur. Control Conf. ECC 2015*, vol. 7, no. 6, pp. 648–653, 2015.

[18] Q. R. Hamid and J. A. Barria, "Congestion Avoidance for Recharging Electric Vehicles Using Smoothed Particle Hydrodynamics," *IEEE Trans. Smart Grid*, vol. 31, no. 2, pp. 1014–1024, 2016.

[19] S. Martinenas, K. Knezovic, and M. Marinelli, "Management of Power Quality Issues in Low Voltage Networks using Electric Vehicles: Experimental Validation," *IEEE Trans. Power Deliv.*, vol. 32, no. 2, pp. 971–979, 2016.

[20] A. T. Procopiou, J. Quiros-Tortos, and L. F. Ochoa, "HPC-Based Probabilistic Analysis of LV Networks with EVs: Impacts and Control," *IEEE Trans. Smart Grid*, vol. 8, no. 3, pp. 1479–1487, 2017.

[21] C. Kattmann, K. Rudion, and S. Tenbohlen, "Detailed power quality measurement of electric vehicle charging infrastructure," *CIRED - Open Access Proc. J.*, vol. 2017, no. 1, pp. 581–584, 2017.

[22] K. Hou *et al.*, "A Reliability Assessment Approach For Integrated Transportation and Electrical Power Systems Incorporating Electric Vehicles," *IEEE Trans. Smart Grid*, vol. 9, no. 1, pp. 1–1, 2016.

[23] K. S. Ko and D. K. Sung, "The Effect of EV Aggregators with Time-Varying Delays on the Stability of a Load Frequency Control System," *IEEE Trans. Power Syst.*, vol. 33, no. 1, pp. 1–1, 2017.

[24] N. Banol A., S. Hashemi, P. Bach Andersen, C. Træholt, and R. Romero, "V2G Enabled EVs Providing Frequency Containment Reserves: Field Results," *2017 IEEE Int. Conf. Ind. Technol.*, p. 6, 2018.

[25] Y. Huo, F. Bouffard, and G. Joós, "An Energy Management Approach for Electric Vehicle Fast Charging Station," 2017.

[26] S. Negarestani, M. Fotuhi-Firuzabad, M. Rastegar, and A. Rajabi-Ghahnavieh, "Optimal Sizing of Storage System in a Fast Charging Station for Plug-in Hybrid Electric Vehicles," *IEEE Trans. Transp. Electrif.*, vol. 2, no. 4, pp. 443–453, 2016.

[27] M. Gjelaj, C. Træholt, S. Hashemi, and P. B. Andersen, "Optimal design of DC fast-charging stations for EVs in low voltage grids," *2017 IEEE Transp. Electrif. Conf. Expo, ITEC 2017*, pp. 684–689, 2017.

[28] M. Gjelaj, S. Hashemi, C. Træholt, and P. B. Andersen, "Grid Integration of DC Fast-Charging Stations for EVs by using Modular Li-ion Batteries," *IET Gener. Transm. Distrib.*, 2018.

[29] M. Gjelaj, C. Traholt, S. Hashemi, and P. B. Andersen, "Cost-benefit analysis of a novel DC fast-charging station with a local battery storage for EVs," *2017 52nd Int. Univ. Power Eng. Conf.*, pp. 1–6, 2017.

[30] M. A. Hannan, M. M. Hoque, A. Hussain, Y. Yusof, and P. J. Ker, "State-of-the-Art and Energy Management System of Lithium-Ion Batteries in Electric Vehicle Applications: Issues and Recommendations," *IEEE Access*, vol. 3536, no. c, pp. 1–1, 2018.

[31] B. Nykvist and M. Nilsson, "Rapidly falling costs of battery packs for electric vehicles," *Nat. Clim. Chang.*, vol. 5, no. 4, pp. 329–332, 2015.

[32] Nordhaven project:, "Design - dimensioning of the energy infrastructure of future sustainable cities," http://energylabnordhavn.weebly.com/ , Copenhagen, 2018.

[33] International Electrotechnical Commission (IEC) standard, "IEC 61851: Conductive charging systems for EV, version 2017." .

[34] International Electrotechnical Commission (IEC) standard, "IEC 15118: Vehicle to grid communication interface within the power systems, version 2018."

[35] International Electrotechnical Commission (IEC) standard, "IEC 62196 : Connectors for conductive charging of electric vehicles, version 2017." .

[36] DTU Elektro, "Electric Vehicle Lab: Electric vehicle power system integration', http://www.powerlab.dk/Facilities/Electric-Vehicle-Lab."

[37] ABB, "High-Power Electric Vehicle Fast Charging Station, report 2018," https://new.abb.com/ev-charging/products/car-charging/high-power-charging.

[38] H. Christiansen, "Documentation of the Danish National Travel Survey," no. August, 2016.

[39] M. Fosgerau, K. Hjorth, T. C. Jensen, and N. Prameswari, *Prediction model for travel time variability*. 2016.

[40] Shell, "Copenhgen: Annual report of users' refuelling behaviour," https://www.shell.dk/refuelling/behaviour, 2017, 2017.

[41] IEA: International Energy Agency, "Technology Roadmap - Electric and Plug-in Hybrid Electric Vehicles, 2017."

[42] D. Boardman, A., Greenberg, D., Vining, A. and Weimer, *Cost Benefit Analysis: Concepts and Practice*, 4th Editio. 2018.

[43] Y. Cao, C. Li, X. Liu, B. Zhou, C. Y. Chung, and K. W. Chan, "Optimal scheduling of virtual power plant with battery degradation cost," *IET Gener. Transm. Distrib.*, vol. 10, no. 3, pp. 712–725, 2016.

[44] B. Xu, A. Oudalov, A. Ulbig, G. Andersson, and D. S. Kirschen, "Modeling of lithium-ion battery degradation for cell life assessment," *IEEE Trans. Smart Grid*, vol. 9, no. 2, pp. 1131–1140, 2018.

[45] N. Takami, H. Inagaki, Y. Tatebayashi, H. Saruwatari, K. Honda, and S. Egusa, "High-power and long-life lithium-ion batteries using lithium titanium oxide anode for automotive and stationary power applications," *J. Power Sources*, vol. 244, pp. 469–475, 2013.

[46] B. Kaun and S. Chen, "Cost-Effectiveness of Energy Storage in California: Application of the Energy Storage Valuation Tool to Inform the California Public Utility Commission Proceeding," *EPRI Energy Storage Valuat. Tool California, Palo Alto*, p. 10, 2015.

[47] Montell & Partners, "Energimarknadsinspektionen: Framtagande av kalkylränta för en skälig avkastning för elnätsföretagen för perioden 2016-2019 [online]. Available: http://ei.se/Documents/Forhandsreglering_el/2016_2019/Dokument/Framtagande_av_kalkylranta_for_en_ skalig_avkas."